Title

1.7-micron Optical Coherence Tomography Angiography for diagnosis and monitoring of Hereditary Hemorrhagic Telangiectasia - A pilot study

Journal

IEEE Transactions on Biomedical Engineering, PP(99)

ISSN

0018-9294

Authors

Murthy, Raksha Sreeramachandra
Elsanadi, Rachel
Soliman, John
et al.

Publication Date

2024-10-10

DOI

10.1109/tbme.2024.3473871

1.7-micron Optical Coherence Tomography Angiography for diagnosis and monitoring of Hereditary Hemorrhagic Telangiectasia - A pilot study

Raksha Sreeramachandra Murthy, Rachel Elsanadi, John Soliman, Yan Li, Li-Dek Chou, Dennis Sprecher , Kristen M. Kelly, Zhongping Chen, *Member, IEEE*

***Abstract*— *Objective:* Develop a multi-functional imaging system that combines 1.7µm optical coherence tomography/angiography (OCT/OCTA) to accurately interrogate Hereditary Hemorrhagic Telangiectasia (HHT) skin lesions. *Methods:* The study involved imaging HHT skin lesions on five subjects including lips, hands, and chest. We assessed the attributes of both HHT lesions and the healthy vasculature around them in these individuals, employing quantifiable measures such as vascular density and diameter. Additionally, we performed scans on an HHT patient who had undergone anti-angiogenic therapy, allowing us to observe changes in vasculature before and after treatment. *Results:* The results from this pilot study demonstrate the feasibility of evaluating the HHT lesion using this novel methodology and suggest the potential of OCTA to non-invasively track HHT lesions over time. The average percentage change in density between HHT patients' lesions and control was 37%. The percentage increase in vessel diameter between lesion and control vessels in HHT patients was 23.21%. *Conclusion*: In this study, we demonstrated that OCTA, as a functional extension of OCT, can non-invasively scan HHT lesions in vivo. We scanned five subjects with HHT lesions in various areas (lip, ear, finger, and palm) and quantified vascular density and diameter in both the lesions and adjacent healthy tissue. This non-invasive method will permit a more comprehensive examination of HHT lesions. *Significance:* This method of non-invasive imaging could offer new insights into the physiology, management, and therapeutics of HHT-associated lesion development and bleeding.**

***Index Terms*— Optical Coherence Tomography, Hereditary Hemorrhagic Telangiectasia, Dermatology, OCT Angiography.**

I. Introduction

Hereditary hemorrhagic telangiectasia is an inherited disorder that causes abnormal connections between arteries and veins. It is estimated to affect approximately 1.5M people globally [1]. Larger lesions are called arteriovenous malformations (AVM) and most commonly occur in the lungs and brain and can be complicated by stroke and brain abscess. Smaller lesions, also involving capillary overgrowth can be telangiectasias or small AVMs and typically occur on external surfaces, including the mucosa and skin. The disease is caused by mutations in genes that are associated with TGFβ signaling, with over 95% involving the TGFβ receptors ALK1 and endoglin. Studies in mice [2] have shown that the formation of lesions appears to correlate with active angiogenesis, and this is consistent with the frequent presence of telangiectasias in so-called "high traffic" areas such as lips, tongue, fingertips, and the nasal mucosa.

In light of these findings, the anti-angiogenic bevacizumab (Avastin), which is a neutralizing antibody to VEGF, was tried in patients, first as off-label administration to a few patients and then later in historically controlled trials, where it showed success in reducing nosebleeds (epistaxis) [3-5]. In HHT patients, these can be frequent, high volume, and of long duration, and are extremely debilitating both due to the loss of blood (and reduced hemoglobin levels) and to the social stigma. Improvement in liver disease associated with liver AVMs has also been reported [6,7]. Orally available anti-angiogenic Pazopanib in preliminary studies has shown dramatic benefits in epistaxis and GI bleeding (above 80% response), while Pomalidomide has shown at least 60% response rates [8].

Interestingly, despite these dramatic findings, there is still no clear consensus on why these reagents prevent bleeding. The primary school of thought is that inhibition of VEGF signaling will both block the creation of neo vasculature (thereby blocking the formation of new telangiectasias and AVMs), and potentially involute abnormal vessels already present in vulnerable tissue and at the mucosal or skin surface. The problem has always been the lack of an easy and effective way to observe changes in the vasculature in patients receiving drugs. Specifically, it's difficult to determine whether there's a lack of new vessel growth and a corresponding decrease in future bleeding, if lesion vessels are collapsing, resulting in a loss of vascular density (known as rarefaction), or if the remaining vessels are stabilized against fracture. An advantage we do have, and one we plan to leverage in this study, is that some of the lesions often are on the skin surface, and more typically on mucosal surfaces making them amenable to

This work was supported in part by the National Institute of Health (R01EB-030558, R01HL-125084, R01EY-028662, R01EB-030024) and Air Force Office of Scientific Research (FA9550-20-1-0052) grants.

R.S, Z.C are affiliated with the Department of Biomedical Engineering, University of California, Irvine and the Beckman Laser Institute, University of California, Irvine, CA 92697 USA. Y.L, L.C are affiliated with the Beckman Laser Institute, University of California, Irvine, CA 92697 USA. R.E, J.S, K. K are affiliated with the Department of Dermatology, University of California, Irvine, CA 92697 USA. D.S is affiliated with the HHT foundation, Monkton, MD 21111 USA (correspondence e-mail: z2chen@uci.edu).

imaging. Therefore, we have developed a 1.7 µm OCT/OCTA enabling accurate diagnosis and non-invasive monitoring of lesion size in HHT patients over time.

Various devices are available to observe and measure vascular density, and each likely has elements of value for specificity and accuracy. However, OCT has the potential to provide the best combination of benefits because of its high-resolution (1-15 µm), its real-time cross-sectional imaging with a penetration depth of 1-2 mm, and its safe, non-invasive operation. Furthermore, our group has developed Doppler OCT/OCTA to visualize vascular networks and angiogenesis [9,10]. Integrated OCT and OCTA imaging can provide information on lesion architecture and microvasculature.

Recently, several groups have applied OCTA technology to image macular telangiectasia [11-14]. However, very few studies describe the application of OCT in skin telangiectasia [15-17]. Taudorf et al utilized a commercially available Vivosight OCT to characterize facial telangiectases before and during intense pulsed light (IPL) treatment [15]. The study discusses the benefit of combining Doppler OCT imaging to monitor IPL treatment for vascular skin disorders. Despite their capability to perform pre- and post-IPL treatment vasculature scans, they observed no discernible alterations in vessel width or attenuation throughout the duration of the treatment process using the commercial VivoSight OCT system. Dynamic OCT was used to reliably capture superficial cutaneous blood vessels in both cross-sectional and en face images [18,19]. Cardinell et al demonstrate that OCTA can measure several quantitative parameters such as vascular density, lesion area, and fractal dimension of superficial as well as deep HHT lesions using the VivoSight system [17]. However, the correlation between these vascular parameters and HHT disease at different stages as well as response to different treatments is not well characterized. Various external factors such as the effect of temperature affected the lesion characteristics. Another main challenge was the slow image acquisition, where a single scan lasted for 3 minutes. This extended acquisition time significantly increased the susceptibility to motion artifacts.

Conventional 1.3-micron OCT systems used in imaging HHT lesions typically achieve imaging depths of approximately 1 mm in skin [15]. A 1.7-micron system offers potential for deeper penetration, which could be beneficial for imaging HHT lesions on the skin due to several factors related to the nature of these lesions. Cutaneous HHT lesions are small, dilated blood vessels that can be located at varying depths ranging from 1- 2 mm within the skin [1, 20] potentially extending beyond the reach of conventional OCT systems. To accurately visualize and assess these lesions, particularly in patients with multiple or complex presentations, the OCT system must penetrate deeper into the skin layers where these abnormalities reside. The ability to capture images at different depths enhances the overall understanding of the vascular architecture and the extent of the lesions, as well as their potential involvement with surrounding tissues. Furthermore, deeper imaging can help in identifying lesions that are not readily visible on the skin surface, thereby improving the diagnostic capabilities of OCT systems in evaluating HHT. Deeper penetration is essential for comprehensive imaging of HHT lesions, enabling clinicians to provide better care and management for affected patients.

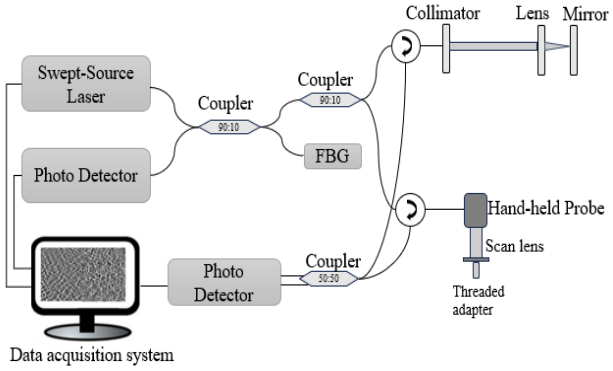

Fig. 1. Schematic representation of 1.7-micron OCT/OCTA system

Our group has applied 1.7µm OCT system in dermatology, gynecology, and cardiology [21-23]. The 1.7µm laser improves penetration depth by 25% compared to the conventional 1.3µm systems and commercially available OCT systems [22,23]. In this study, we report a 1.7µm OCT/OCTA imaging system with enhanced depth penetration, which proves valuable for the non-invasive imaging of HHT lesions by visualizing morphology and vasculature in deeper layers of the skin. We have captured images of various lesions, including those on the hand, lip, ear, and chin as an initial assessment of this technology for cutaneous imaging. In addition, our research pilots the effectiveness of OCT in studying the evolving impacts of Anti-VEGF treatment. Finally, we conduct a comparative analysis to discern the morphological parameter disparities between HHT lesions and control subjects, focusing on the variations from healthy vasculature.

II. Methods

A. System setup

The schematic representation of the 1.7 µm OCT/OCTA is as shown in fig 1. The system consists of a Mach-Zehnder interferometer (MZI) with a 1.7 µm center wavelength-swept light source (Santec, Inc. HSL-40-90-B, 90 kHz, 120 nm bandwidth). The output energy is split by a 90:10 coupler. 90% of the energy is supplied to the sample arm and the remaining 10% is supplied to the reference arm. The system is equipped with a Fiber Bragg Grating (FBG) to increase phase stability by providing a precise wavelength trigger [24]. It reduces trigger jitter, synchronize the OCT signal, leading to more accurate and reliable phase-resolved imaging. The reference arm consists of a collimator, lens, and mirror. The sample arm supplied with 90% energy consists of a hand-held probe with a threaded adapter to adjust the focal length. The handheld probe is equipped with a dual-axis galvanometer and a scan lens for 3D OCT imaging. Two custom-built circulators (Santec Holdings Corp) with a center wavelength of 1650 nm are used to separate the illumination light and back reflected light. The interference signal generated by the sample and reference arm in the 50:50

This article has been accepted for publication in IEEE Transactions on Biomedical Engineering. This is the author's version which has not been fully edited and content may change prior to final publication. Citation information: DOI 10.1109/TBME.2024.3473871

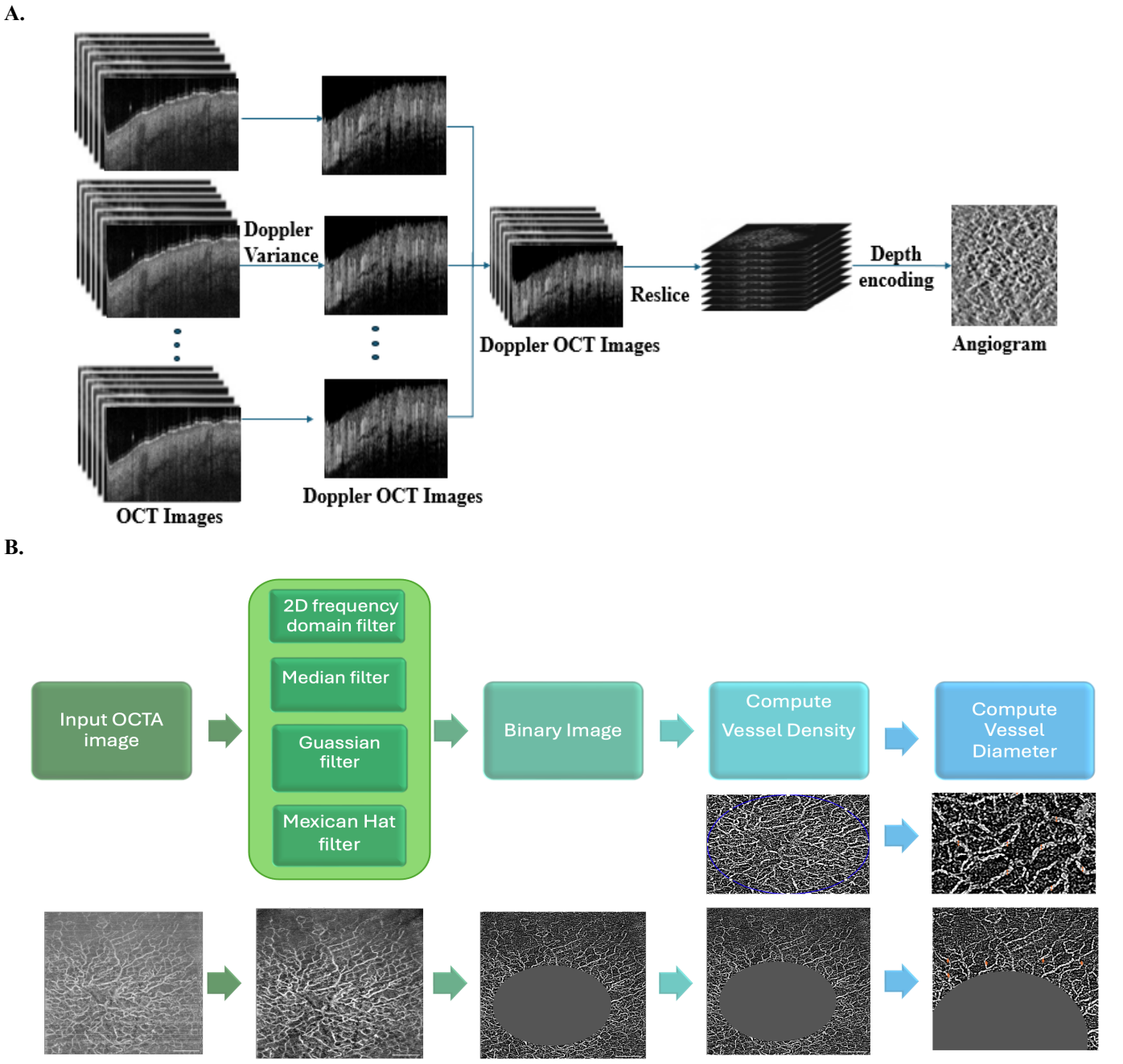

Fig. 2(A). Scanning protocol. (B). Flowchart illustrating the image processing steps: The process includes the following stages: acquisition of OCTA images, application of filtering operations, conversion to a binary image, computation of vessel density within the region of interest (HHT lesions) and surrounding healthy tissue, and calculation of vessel diameter at various points in the vessels (marked in red).

coupler is detected by a balanced photodetector. The data acquisition software is written in C++ which allows for faster data processing and real-time displaying of images.

B. Scanning protocol

In this study, an interframe scanning protocol is applied to extract vascular information. This technique involves capturing multiple cross-sectional images (B-scans) at the same position over time. Specifically, 6 B-scan images are acquired during the image acquisition process at the same spatial location as shown in Fig. 2A. Intensity-based Doppler variance algorithm is applied to obtain Doppler OCT images [25]. Doppler OCT images are re-sliced along depth direction to obtain enface OCTA images. The entire imaging area is 6 mm × 6 mm.

C. In vivo human experiment

The experiments were carried out in accordance with the protocol approved by the Institutional Review Board at the University of California, Irvine. 5 HHT patients and 5 healthy

This article has been accepted for publication in IEEE Transactions on Biomedical Engineering. This is the author's version which has not been fully edited and content may change prior to final publication. Citation information: DOI 10.1109/TBME.2024.3473871

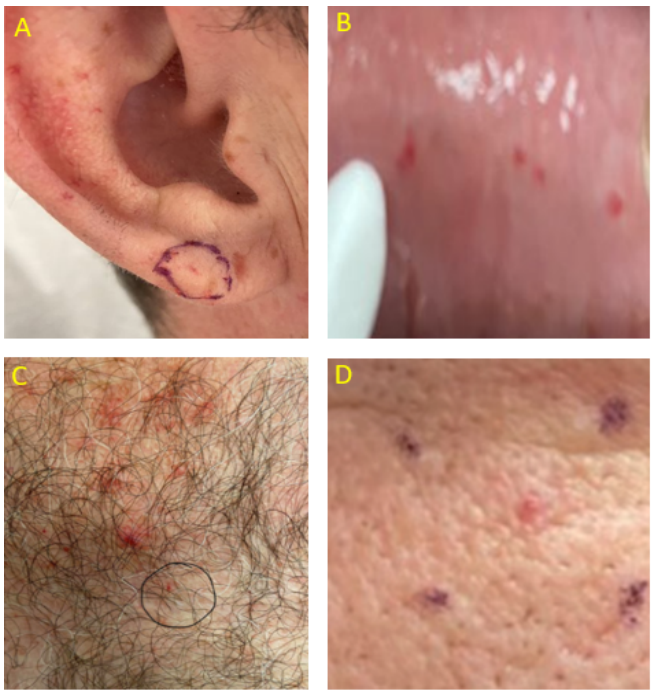

Fig 3. HHT lesions of patients. (A). Ear (B). Lip (C). Chest (D). Chin

subjects were recruited from the Department of Dermatology, University of California, Irvine. The patients with skin telangiectasia including lip, ear, palm, and hand were scanned using 1.7- µm OCT/OCTA. Fig. 3 shows illustrative clinical images of telangiectases of the patients. Among 5 patients with HHT, one individual with a HHT lesion in the chest region (Fig 3c) received anti-angiogenic bevacizumab therapy. We scanned this patient before and 6 months after undergoing the treatment.

Since various external factors such as the effect of temperature influence the lesion characteristics, the subjects were imaged 10-15 minutes post arrival at the imaging site to maintain constant body temperature. To obtain consistent and reliable data, it is crucial to standardize imaging conditions such as temperature. Variations in temperature can lead to significant changes in the appearance and measurements of HHT lesions, complicating the assessment of lesion progression or response to treatment [17]. By controlling for temperature, we were able to more accurately track changes in lesions over time and in response to treatment, thereby improving the reliability of quantitative assessments in HHT studies. Individual lesion imaging took approximately 30 seconds and caused no discomfort. The handheld probe was sterilized after application on each subject. The imaging area of the HHT subjects included the lesion area as well as the adjacent healthy tissue. As for healthy subjects, the scanning was done on the palm as the dense vascular tissues were easily visible through the OCTA system.

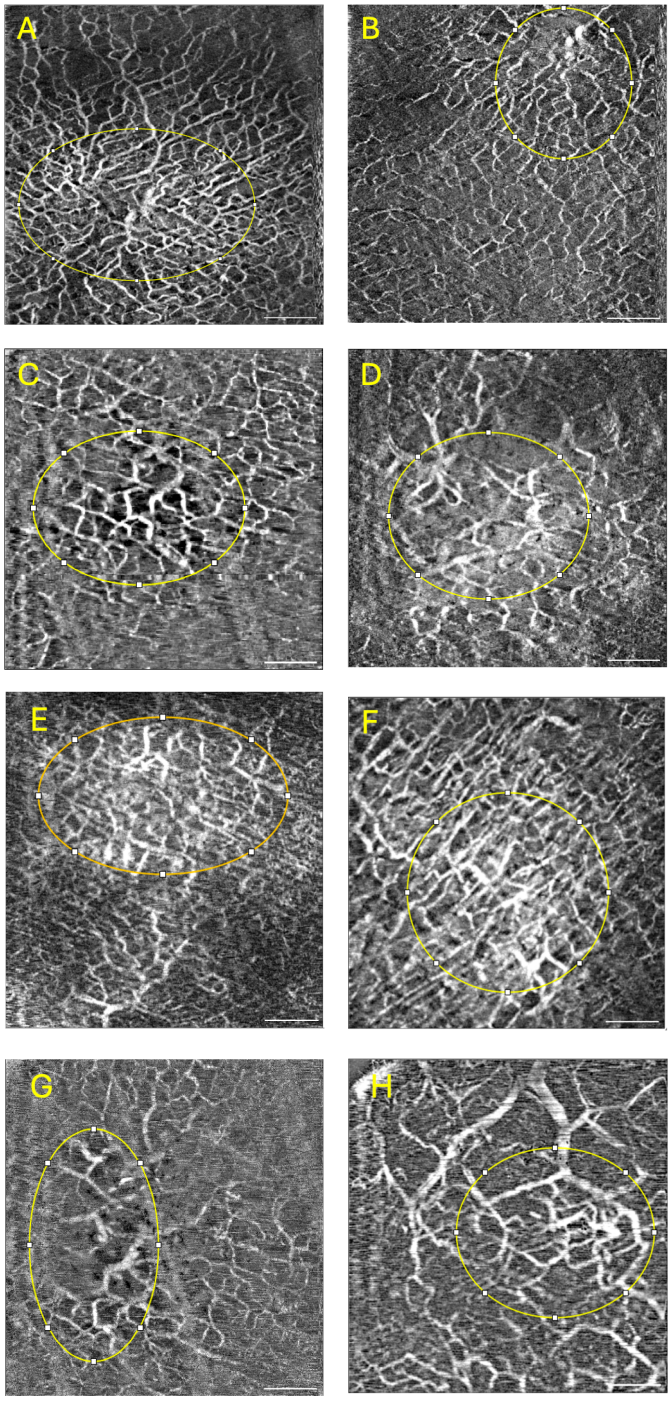

Fig 4. OCTA images of HHT lesions found in various locations on patients, including (A). Palm (B). Palm (C). Finger (D). Lip (E). Ear (F). Hand (G). Chin (H). Lip. These images highlight the characteristic appearance of HHT lesions across different anatomical sites. Scale bar = 1 mm.

D. Image processing

The image processing steps are depicted in Fig. 2B. Vessel density and diameter are calculated using MATLAB and ImageJ software to analyze the OCTA images. Since the data acquisition session takes 30 seconds to complete, motion artifacts are encountered in the OCTA images during acquisition. These artifacts are removed by applying a 2D filter in the frequency domain to the enface OCTA image and

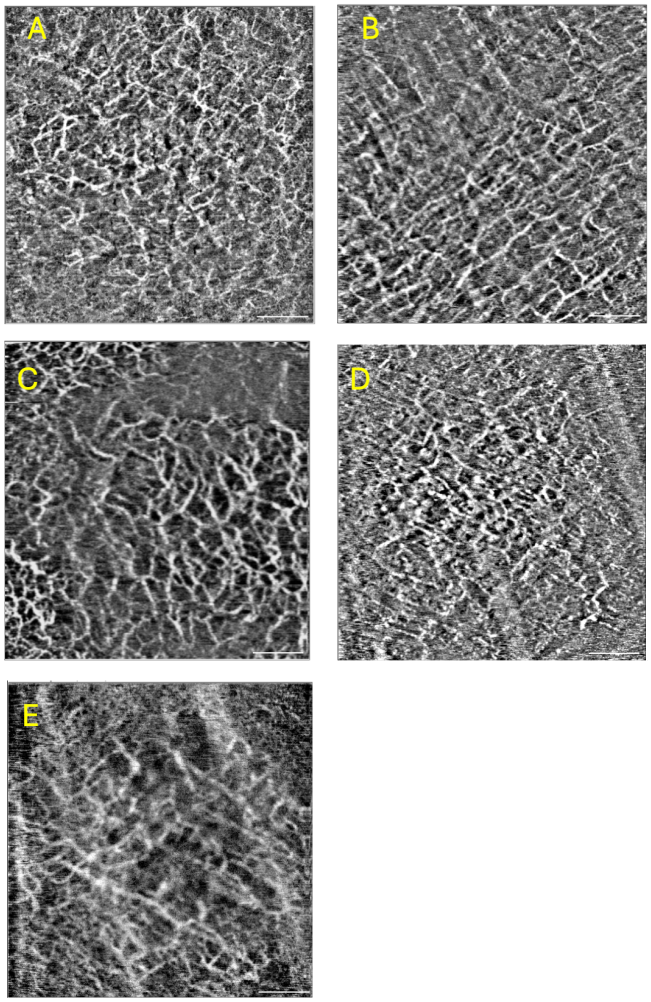

Fig 5. OCTA images of healthy human palms. These images provide a detailed visualization of the microvascular structures within the palms, highlighting the normal vascular patterns observed in healthy individuals. Scale bar = 1 mm.

converting back to the spatial domain. Additionally, median and Gaussian filters are applied to the enface OCTA images. These filtering processes effectively removes the motion artifacts and improves the image quality. Following this, a Mexican-hat filter is then applied to these images to enhance vessel contrast and definition. The images are then converted to binary images. Vessel density is computed by analyzing the lesion area within the defined Region of Interest (ROI) and comparing it to the adjacent tissues in the enface images. To determine the mean vessel diameter, multiple vessels are measured, and the results are averaged to provide a representative value for vessel diameter within the imaged area. This comprehensive approach ensures that the vessel density and diameter measurements are accurate and reliable, providing valuable quantitative data for assessing the vascular characteristics of the lesions.

E. Quantitative analysis of OCTA images

The 6×6 mm images reveal the densely concentrated network of the dilated and interconnected vasculature of the telangiectasia, as well as the supporting vessels compared to healthy subjects. The OCTA images of 5 HHT subjects are

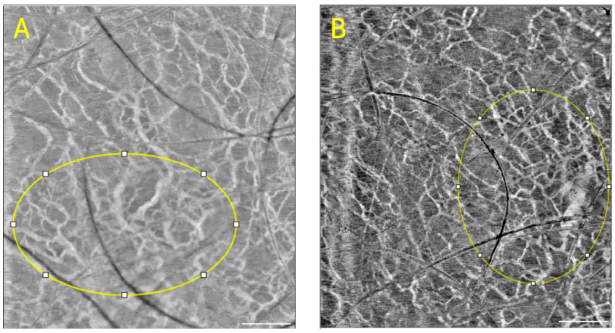

Fig. 6. OCTA images of HHT subject's chest area (A) pre- and (B) post-anti-angiogenic therapy. Scale bar measures 1 mm.

shown in Fig. 4. The vascular density and diameter are quantified in Table 1. In HHT patients, the average vessel density of the lesion vessels was 67.44% and the control vessel density was 42.05%. The average vessel diameter of lesion vessels in HHT subjects was 81.48±7.62. The average control vessel diameter was 62.82±12.51μm.

We also conducted a comparison between the vasculature of individuals with HHT and that of healthy human subjects. To account for potential variations in vasculature across different sites, we specifically compared the palms of healthy humans with those of HHT subjects. The mean vessel density for healthy human subjects' palms was 57.36%, with a mean vessel diameter of 57.28±7.60 μm. In Fig 5, OCTA images of palms from five healthy subjects are presented. The vascular density and diameter are quantified in Table 2. A 16.20% change in vessel density and a 25.44% change in vessel diameter were observed between the palms of HHT subjects and healthy humans. One out of the five patients with hereditary hemorrhagic telangiectasia (HHT) received anti-angiogenic bevacizumab therapy, resulting in reduced bleeding. OCTA images were obtained pre- and post-bevacizumab therapy. The vascular density and diameter are quantified in Table 3. Figures 6a and 6b depict the lesion in the patient before and after bevacizumab therapy, revealing a 36% reduction in lesion vessel density and a 20.9% decrease in lesion vessel diameter.

Additionally, uninvolved vessel density and diameter decreased by 16.29% and 34.29%, respectively post-therapy.

III. Discussion

OCTA elucidates the vascular changes on the skin surface. The quantitative assessment provides an in-depth idea of the vascular density and diameter of the HHT lesions and adjacent vessels on the surface of the skin. The lesion vessel density and diameter among HHT subjects were 37.45% and 23.21% more compared to the adjacent vessels. These data offer us a quantitative path towards following changes during a systemic intervention. As a case study, we were able to apply this technique to one patient before and after therapy, targeting the very same lesion with the same analytic tool. This recommends the feasibility of this application. It is of interest that a change in density and diameter after bevacizumab therapy was observed.

TABLE I
QUANTITATIVE ANALYSIS OF HHT SUBJECTS

HHT Subj-ects	Scan area	Vessel density Control (%)	Vessel density Lesion (%)	Vessel diameter Control (μm)	Vessel diameter Lesion (μm)
P1	Palm	39.887	80.518	48.1±10.9	74.0±13.3
P1	Palm	36.95	71.11	49.0±9.9	72.5±13.0
P2	Chest	62.24	86.5	69.1±18.3	77±14.4
P3	Finger	41.31	61.206	76.18±30.8	83.33±15.3
P3	Lip	37.58	61.98	63.22 ±8.4	88.28±24.3
P3	Ear	43.05	62.6	56.75±22.1	77.38 ±27.8
P4	Finger	36.54	61.001	58.4±22.5	77.5±29.4
P4	Chin	44.4	61.05	58.4 ± 17.9	88.8 ± 34.9
P5	Lip	36.54	61.001	86.3±45.6	94.6 ±22

TABLE II
QUANTITATIVE ANALYSIS OF HEALTHY SUBJECTS DATA

Healthy Subjects	Scan area	Vessel density (%)	Vessel diameter (μm)
S1	Palm	51.59	57.4± 10.9
S2	Palm	56.14	46.7± 15.8
S3	Palm	56.957	65.4± 18.0
S4	Palm	57.471	53.4± 13.5
S5	Palm	64.67	63.5± 24.7

TABLE III
QUANTITATIVE ANALYSIS OF HHT PATIENT'S CHEST DATA BEFORE AND AFTER ANTI-ANGIOGENIC THERAPY

	Vessel density Control (%)	Vessel density Lesion (%)	Vessel diameter Control (μm)	Vessel diameter Lesion (μm)
Pre-treatment	62.24	86.5	69.1±18.3	77±14.4
Post-treatment	52.103	55.259	45.4±13.2	60.9±19.5

The pathologic evaluation of biopsy tissue in HHT patients has noted the dilation of these vessels and their increase in microvascular density [20]. Ten lesions were interrogated of progressively larger size of which 4 were modeled using computer simulation. The assumption is that these lesions evolve over time. The earliest lesion they detected had focally dilated postcapillary venules, which connected to dilated arterioles. Subsequently, the capillaries disappeared, and a direct AV communication was formed with development of a lymphocytic infiltrate. These direct connections intensified over time leading to a dense fabric of arterialized tissue. This process was consistent with the known arterialization of the localized venous system.

Increased VEGF expression, a known feature of HHT physiology, drives neovascularization and thereby increases vascular density. VEGF directed vessel sprouting, and the creation of endothelial tubes is a known outcome of HHT biology. The expectation is that inhibition of VEGF signaling will limit further sprouting, which has merit in preventing the phenotype from becoming worse, but itself should not alter bleeding. Therefore, some modification of the present vessels must be occurring to observe the clinical benefit. The expectation of increased vascular density and vascular diameter from both the biology of HHT as well as the pathologic specimens from HHT patients are consistent with the findings from OCT in this report. Such parallel findings offer some substantiation for the value and relevancy of this OCT non-invasive approach.

Recent reports have attempted to explain the common manifestation of elevated blood pressure when administering systemic anti-VEGF compounds [26]. The most compelling case has been the notion that small resistance-related vessels, pivotal to the development of HTN, are rendered either under-perfused, or under-represented due to their absence or collapse leading to enhanced peripheral resistance and thus higher blood pressures. VEGF inhibition is thought to limit Nitrous Oxide production and enhance endothelin 1 leading to reduction in flow. This occurrence of "rarefaction" might also occur in HHT lesions, and possibly, preferentially, given their thin walls and relevant prostaglandin- induced vascular collapse. This absence of small capillaries, and thus lowering of the density of lesions, could explain the reduction in the arterial pressure leading to reduced frequency, intensity and potentially duration of bleeds. These attributes could explain the benefit to the HHT patient [3, 27].

The availability of a non-invasive tool to evaluate the in-vivo vascular structure of HHT lesions will be instructive for determining heterogeneity among various topographical regions, inter-individual variation, and evolution with time. Rather than the more burdensome invasive tissue biopsy approach, OCT non-invasive technology can better elucidate the vascular relevance of a test treatment to the clinical outcome. For example, if rarefaction is indeed one of the mechanisms for anti-VEGF drug influence, we might observe a change in density and/or vessel diameter as suggested in our one pre- and post-treatment patient example.

In addition, a pilot read of a pharmaceutical at its treatment initiation may offer predictive advantages. We might anticipate that the degree to which a pharmacologic intervention would modify the peripheral telangiectatic lesions may infer the degree to which there will be concurrent benefit for bleeding at less image-accessible sites, such as the nose or GI tract. In this way, OCT may help predict the value of an HHT therapeutic. This approach therefore represents a treatment opportunity at the initial trial period of drug administration.

There are limitations to the outcome of this study. The current study has limited HHT patient enrollment and does not characterize the patients with variation in vital signs, medical history, as well as age or gender. The limited availability of HHT patients hinders comprehensive analysis. However, the uniformity of the results among our 5 HHT patients and among their skin lesion of various locations, as well as the results from our control subjects to some degree mitigates against these patient traits as substantial variables. Perhaps more critical is the need to precisely identify the location within the lesion being interrogated, as that may influence results. Once again, our uniformity of findings does question the relevance of this factor as well. In addition, we chose to interrogate lesions only on the skin surface, and none on mucosal surfaces which may have a different morphology. Lesions can be found on the tongue or on the anterior septum of the nose. This may pose technical challenges because utilizing OCT for imaging mucosal surfaces necessitates the use of an endoscopic probe and meticulous imaging of the site due to its delicate nature. It is also possible that lesions were extended beyond the imaging

capability of the instrument, thus not completely representing the 3D perspective of such a lesion. Otherwise, OCT can capture detailed, 3D cross-sectional images of biological tissues. However, its resolution and penetration depth may have limitations, especially when imaging deeper tissues.

IV. Conclusion

In this study, we demonstrated that a 1.7 μm OCTA, as a functional extension of OCT, can be used to non-invasively scan cutaneous HHT lesions in vivo, with an increase in penetration depth compared to conventional 1.3 μm OCTA. We scanned 5 subjects with HHT lesions in different areas including lip, ear, finger, and palm. We were able to quantify the vascular density and diameter of lesions and adjacent healthy tissue. In the future, we will both further refine this methodology and apply it to a more comprehensive cohort of HHT patients. In summary, we developed a technical methodology and demonstrated the feasibility for OCT assessment of HHT skin lesions, we propose that this non-invasive method will permit a more comprehensive examination of HHT lesions, a more thorough analysis of their heterogeneity, and afford an approach towards interrogating longitudinal changes. This might represent a major advance for evaluating and understanding HHT management and therapeutics.

References

[1]. C.L. Shovlin, "Hereditary haemorrhagic telangiectasia: pathophysiology, diagnosis and treatment." *Blood Rev,* vol. 24, no. 6, pp. 203-219, Nov. 2010.

[2]. S. Tual-Chalot, S. P. Oh, and H. M. Arthur, "Mouse models of hereditary hemorrhagic telangiectasia: recent advances and future challenges," *Front Genet,* vol. 6, pp. 25, 2015.

[3]. V.N Iyer, et al. "Intravenous Bevacizumab for Refractory Hereditary Hemorrhagic Telangiectasia-Related Epistaxis and Gastrointestinal Bleeding." *Mayo Clinic proceedings*, vol. 93, no. 2, pp. 155-166, Mar 2018.

[4]. H. Al-Samkari et al. "Systemic bevacizumab for the treatment of chronic bleeding in hereditary haemorrhagic telangiectasia," J Intern Med, vol. 285, no. 2, pp. 223–231, Feb. 2019.

[5]. H. Al-Samkari, "Systemic Bevacizumab for Hereditary Hemorrhagic Telangiectasia: Considerations from Observational Studies," *Otolaryngol Head Neck Surg*, vol. 160, no. 2, p. 368, Feb. 2019.

[6]. S. Dupuis-Girod, I. Ginon I, J. C. Saurin, et al. "Bevacizumab in patients with hereditary hemorrhagic telangiectasia and severe hepatic vascular malformations and high cardiac output," *JAMA*, vol. 307, no.9, pp. 948-955, Mar. 2012.

[7]. A. Guilhem, A. E. Fargeton, A. C. Simon, et al. "Intra-venous bevacizumab in hereditary hemorrhagic telangiectasia (HHT): A retrospective study of 46 patients," *PLoS One*, vol. 12, no.11, Nov. 2017.

[8]. S. Shadi et al. "Pomalidomide Reduces Bleeding and Alters Expression of Angiogenesis-Related Proteins in Patients with Hereditary Hemorrhagic Telangiectasia." *Blood*, vol. 134, no. 1, pp.5761-5761, Nov. 2019.

[9]. G. Liu et al. "In vivo, high-resolution, three-dimensional imaging of port wine stain microvasculature in human skin." Lasers Surg Med. vol. 45, no. 10, pp. 628-632, Dec. 2013.

[10]. H. S. Chen, C. H. Liu, W. C. Wu, *et al* "Optical Coherence Tomography Angiography of the Superficial Microvasculature in the Macular and Peripapillary Areas in Glaucomatous and Healthy Eyes," *Invest Ophthalmol Vis Sci*, vol. 58, no. 9, pp. 3637-3645, Jul. 2017.

[11]. L. Chidambara, S. G. Gadde, N. K. Yadav, et al. "Characteristics and quantification of vascular changes in macular telangiectasia type 2 on optical coherence tomography angiography," *Br J Ophthalmol*, vol. 100, no. 11, pp. 1482-1488, Nov. 2016.

[12]. S. Sindhar, et al. "Identification of Retinal Vascular Lesions Using Ultra-Widefield Angiography in Hereditary Hemorrhagic Telangiectasia Patients," Ophthalmol Retina, vol. 3, no. 6, pp. 510-515, Feb. 2019

[13]. R. F. Spaide, J. M. Jr Klancnik, M. J. Cooney, "Retinal vascular layers in macular telangiectasia type 2 imaged by optical coherence tomographic angiography," JAMA Ophthalmol, vol. 133, no.1, pp. 66-73, Jan. 2015.

[14]. Y. Kihara, T. F. C Heeren, C. S. Lee, et al, "Estimating Retinal Sensitivity Using Optical Coherence Tomography With Deep-Learning Algorithms in Macular Telangiectasia Type 2," *JAMA Netw Open*. Vol. 2, no. 2, Feb. 2019.

[15]. Taudorf, H. Elisabeth et al. "Dynamic Optical Coherence Tomography Imaging of Telangiectasia Prior to Intense Pulsed Light Treatment-An Opportunity to Target Treatment?." *Lasers Surg Med,* vol. 53, no.2, pp. 212-218, Feb. 2021.

[16]. T. E. Quirke, G. Rauscher, L. L. Heath, "Laser Treatment of Leg and Facial Telangiectasia", *Aesthetic Surgery Journal*, Vol. 20, no. 6, pp. 465-470, Nov. 2000.

[17]. J. L. Cardinell, J. M. Ramjist, C. Chen, et al. "Quantification metrics for telangiectasia using optical coherence tomography," *Sci Rep*, vol. 12, no. 1, pp. 1805. Feb. 2022.

[18]. J. Olsen, F. H. Birch-Johansen, L. Themstrup, J. Holmes, G. B. E Jemec, "Dynamic optical coherence tomography of histamine induced wheals," *Skin Res Technol*, vol. 24, no. 4, pp. 592-598. Nov. 2018

[19]. M. Ulrich, L. Themstrup, N. de Carvalho, et al. "Dynamic Optical Coherence Tomography in Dermatology," *Dermatology*, vol. 232, no. 3, pp. 298-311, Apr. 2016.

[20]. I. M. Braverman, A. Keh, B. S. Jacobson, "Ultrastructure and three-dimensional organization of the telangiectases of hereditary hemorrhagic telangiectasia," *J Invest Dermatol*, vol. 95, no. 4, pp. 422-427, Oct. 1990.

[21]. Y. Li, R. S. Murthy, Y. Zhu, et al. "1.7-Micron Optical Coherence Tomography Angiography for Characterization of Skin Lesions-A Feasibility Study," *IEEE Trans Med Imaging*, vol. 40, no. 9, pp. 2507-2512, Aug. 2021.

[22]. Y. Li, N. T. Sudol, Y. Miao, et al. "1.7 micron optical coherence tomography for vaginal tissue characterization in vivo," *Lasers Surg Med*, vol. 51, no. 2, pp. 120-126, Feb. 2019.

[23]. Y. Li, J. Jing, E. Heidari, J. Zhu, Y. Qu, and Z. Chen, "Intravascular optical coherence tomography for characterization of atherosclerosis with a 1.7 micron swept-source laser," Sci. Rep., vol. 7, no. 1, p. 14525, Dec. 2017.

[24]. M. T. Tsai, Y. J. Lee, Y. C. Yao, C. Y. Kung, F. Y. Chang, and J. D. Lee, "Quantitative Phase Imaging With Swept-Source Optical Coherence Tomography for Optical Measurement of Nanostructures," IEEE Photonics Technology Letters, vol. 24, no. 8, pp. 640-642, 2012.

[25]. G. Liu, L. Chou, W. Jia, W. Qi, B. Choi, and Z. Chen, "Intensity-based modified Doppler variance algorithm: Application to phase instable and phase stable optical coherence tomography systems," Opt. Exp., vol. 19, no. 12, pp. 11429–11440, Jun. 2011.

[26]. N. Camarda, et. al, "VEGF Receptor Inhibitor-Induced Hypertension: Emerging Mechanisms and Clinical Implications," Curr Oncol Rep, vol. 24, no. 4, pp. 463-474, Apr. 2022.

[27]. S. Dupuis-Girod et al, "Bevacizumab in patients with hereditary hemorrhagic telangiectasia and severe hepatic vascular malformations and high cardiac output," JAMA, vol. 307, no. 9, pp. 948-955, Mar. 2012.